Spin Polarized Auger Electrons: The Xe $M_{4,5}N_{4,5}N_{4,5}$ Case

G. Snell,[1,2] M. Drescher,[1] N. Müller,[1] U. Heinzmann,[1] U. Hergenhahn,[2] J. Viefhaus,[2] F. Heiser,[2] U. Becker,[2] and N. B. Brookes[3]

[1]*Universität Bielefeld, 33501 Bielefeld, Germany*

[2]*Fritz-Haber-Institut der Max-Planck-Gesellschaft, 14195 Berlin, Germany*

[3]*European Synchrotron Radiation Facility, 38043 Grenoble Cedex, France*

(Received 26 December 1995)

The spin polarization of the Xe $M_{4,5}N_{4,5}N_{4,5}$ Auger electrons was measured after photoionization of free atoms by circularly polarized synchrotron radiation at 834.5 eV. Significant polarization effects were found across the whole Auger group. With the hole state orientation determined from the spin polarization of the $M_4\,{}^1S_0$ Auger line the intrinsic Auger parameters were evaluated for all lines. The orientation derived from the ${}^1S_0$ Auger line is consistent with the measured spin polarization of the $3d_{3/2}$ photoline in good agreement with the two-step model of the Auger decay. [S0031-9007(96)00238-4]

PACS numbers: 32.80.Hd, 32.80.Fb

During the past two decades the spin polarization of valence photoelectrons excited by circularly polarized light has been intensively studied [1]. On theoretical grounds it was predicted that Auger electrons could be spin polarized as well [2,3]. However, the use of this effect as an experimental tool was restricted due to the absence of an intense source for circularly polarized radiation with sufficient energy to create oriented inner-shell holes. In this Letter we report about the first spin-resolved measurements on photoelectrons and Auger electrons from deep, inner-shell states, which overcome this difficulty by using the highly circularly polarized soft x-ray radiation of a helical undulator. We show that spin polarization studies of Auger electrons can give valuable information about the radiationless decay mechanisms and indirectly about the photoionization process of inner shells as well.

The spin polarization of Auger electrons is created by the polarization of the initial hole state. Two mechanisms leading to Auger electron spin polarization can be distinguished [2]. Angular momentum conservation results in "transferred polarization," while a final-state interaction between outgoing electron and doubly charged ionic core creates the "dynamical polarization" [4]. While the latter can be created by any kind of particle or photon impact, the former requires excitation by polarized particle impact or by circularly polarized photons. The degree of spin polarization obtained by polarization transfer is much more pronounced in general. In an angle-resolved experiment, the transferred spin polarization vector lies in the "reaction plane" spanned by the propagation vectors of the incoming radiation and the outgoing electrons. Two independent components of the spin polarization vector directions transversal and longitudinal to the outgoing electrons' momentum can be chosen.

The spin polarization transfer in radiationless decays has been studied experimentally on solid alkali metals and free atoms for excitation energies below 30 eV [5,6]. Measurements on free Ba atoms showed the creation of Auger electron polarization due to the hole orientation in the special case of a ${}^1S_0$ final state [6]. As the Auger transition to a ${}^1S_0$ final state proceeds via only one decay channel the spin polarization is independent of the Auger matrix elements; i.e., no information about the dynamics of the Auger decay could be extracted.

The spin polarization transfer present in the Auger decay sensitively test angular momentum coupling models if two-hole state configurations with total angular momentum $J \neq 0$ are involved. To obtain decay processes resulting in these more general two-hole state configurations sufficiently deep lying, oriented primary hole states have to be excited. We used a newly developed apparatus and the very recently commissioned planar helical undulator "Helios I" for high intensity soft x rays at the third generation synchrotron light source ERSF [7] to measure the transversal component of the transferred spin polarization in the Xe $M_{4,5}N_{4,5}N_{4,5}$ Auger decay.

Figure 1 shows the experimental setup. The radiation of Helios I was monochromatized in a spherical grating monochromator of the "dragon type" [8]. Using a bandwidth of $\Delta E \approx 3$ eV and the photon energy $h\nu = 834.5$ eV the flux in the interaction region was approximately 6×10^{12} photons/s per 100 mA ring current (determined using a silicon photodiode). The energy and polarization analysis of the outgoing electrons were performed by a time-of-flight (TOF) spectrometer followed by a Mott polarimeter of the accelerating and decelerating spherical field type [9] operated at 45 kV. The angular acceptance of the spectrometer was approximately $\pm 3°$. The energy resolution $\Delta E/E \approx 10^{-3}$ necessary for studying the Xe *MNN* Auger decay was attained by applying a retarding potential $U_{\mathrm{ret}} = -510$ V to the spectrometer drift tube. This high resolution was accessible as the fast timing (200 ps overall time resolution) was preserved in the Mott polarimeter.

The spin polarization P of the electrons is given by the backscattered intensities I_1 and I_2 counted in multichannel

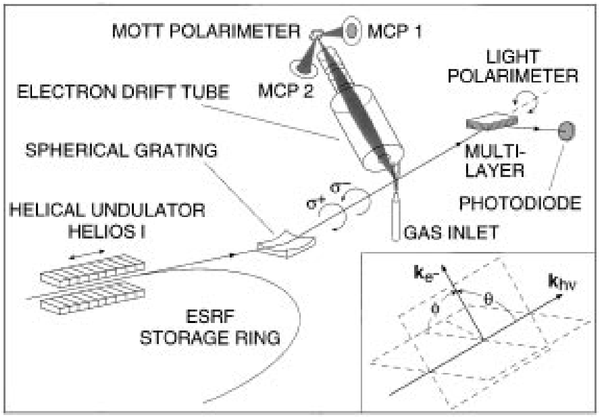

FIG. 1. Experimental setup. The inset shows the geometry of the photoionization process.

plate detector MCP1 and MCP2, respectively, and the polarization sensitivity S_{eff} of the Mott polarimeter:

$$P = \frac{1}{S_{\mathrm{eff}}} \frac{I_1 - I_2}{I_1 + I_2}. \qquad (1)$$

To eliminate instrumental asymmetries, although measured to be smaller than the single statistical error of the measured spin polarization ($\pm 3\%$), successive measurements with left- and right-handed circularly polarized radiation were carried out, taking advantage of the helical undulator's free variability of the light polarization state allowing the production of σ^+, σ^-, and π light [7]. The polarization sensitivity and the detection efficiency of our Mott polarimeter were determined to be $S_{\mathrm{eff}} = -0.27 \pm 0.03$ [10] and $I/I_0 \gtrsim 1 \times 10^{-3}$, respectively, resulting in a figure of merit $S_{\mathrm{eff}}^2 I/I_0 \gtrsim 7 \times 10^{-5}$. Because of the substantial loss of signal intensity during Mott scattering our experiment benefited considerably from the TOF technique's inherent capability of simultaneous acquisition—and in this case additional spin polarization analysis—of all lines in a spectrum. Since for TOF electron spectroscopy a pulsed light source with appropriate timing is essential, the 16-bunch mode of the ESRF storage ring was used. In the *MNN* Auger group the typical integrated count rate was approximately 5 s^{-1}.

For the quantitative interpretation of the measured electron spin polarization the degree of circular polarization of the ionizing radiation has to be known. We determined the light polarization state using W/Si multilayers with 40 periods each 2.0 nm thick as a reflection analyzer [11,12]. By rotating the multilayers azimuthally around the light axis the ellipticity and the spatial orientation of the polarization ellipse were determined. Setting the undulator to produce linearly polarized π radiation the ellipticities measured with a single and a double multilayer reflector, respectively, were compared and the analyzing power of the polarimeter was determined to range from 0.25 to 0.6 depending on the photon energy. Assuming the conservation of the total polarization $P_{\mathrm{tot}} = P_{\mathrm{lin}}(\pi)$ after phase shifting [13], the measurement of the residual linear polarization $P_{\mathrm{lin}}(\sigma)$ when the undulator is set to produce circularly polarized light enabled us to determine the degree of circular polarization: $P_{\mathrm{circ}}(\sigma)^2 = P_{\mathrm{tot}}^2 - P_{\mathrm{lin}}(\sigma)^2$. For photon energies between 680 and 930 eV we measured P_{circ} to range from 0.85 to 0.90. At $h\nu = 834.5$ eV used for the Auger measurements we found $P_{\mathrm{tot}} = 0.95$ and $P_{\mathrm{lin}}(\sigma) = 0.32 \pm 0.04$ resulting in $|P_{\mathrm{circ}}| = 0.89 \pm 0.05$. Within the experimental uncertainties P_{circ} was identical for σ^+ and σ^- radiation. The linear component of the radiation was lying in the horizontal plane. The polarization measurements will be presented in detail elsewhere [14].

The $M_{4,5}N_{4,5}N_{4,5}$ Auger electron spectrum is shown in Fig. 2(a). The assignment of the lines refers to [15]. In order to determine the spin polarization P of the different Auger lines the four measured spectra—according to the signals from MCP1 and MCP2 using σ^+ as well as σ^- light—were used to build spin separated partial intensities $\hat{I}_1$ and $\hat{I}_2$. These spectra, which would correspond to detected intensities I_1 and I_2 in a perfect Mott detector (i.e., $S_{\mathrm{eff}} = 1$), were then

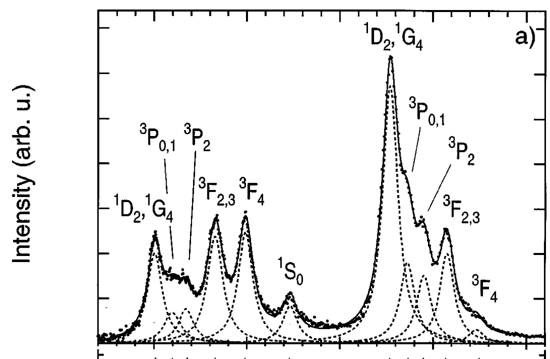

FIG. 2. Xe $M_{4,5}N_{4,5}N_{4,5}$ Auger lines at $h\nu = 834.5$ eV: (a) Intensity spectrum of the *MNN* Auger group with fitted Voigt profiles; (b) ○ measured spin polarization across the Auger spectrum evaluated for each 200 meV kinetic energy interval of the intensity spectrum; ● spin polarization of the individual Auger lines evaluated from the areas of fitted Voigt profiles. The vertical error bars include both the statistical and systematic uncertainties. At low intensities the statistical error dominates. The horizontal bars indicate the fitted linewidths.

fitted with Voigt profiles. Equivalent Voigt profiles fitted into the non-spin-dependent spectrum and their sum are shown in Fig. 2(a). The areas of the fitted Auger lines in $\hat{I}_1$ and $\hat{I}_2$ were then used to determine P. The results agree well with spin polarization values obtained by fitting the four measured spectra (I_1, I_2 for σ^+ and σ^- light) with a sum of Voigt profiles directly. P/P_{circ}, i.e., the spin polarization normalized to the degree of circular polarization, is shown in Fig. 2(b) for the different Auger lines as closed circles. An evaluation of the spin polarization using the total counts in kinetic energy intervals of 200 meV instead of using fitted line areas is plotted in Fig. 2(b) as open circles. Using this method of analysis the spin polarization is averaged over all contributions of lines present at a given kinetic energy. In this way structures in the spin polarization are visualized, which cannot be recognized in the line-fit oriented analysis. Comparing the two different methods of analysis we find good agreement for all lines if we take into account effects from overlapping peaks. This overlap is especially pronounced at 521 and 534.5 eV kinetic energies, where in the continuous evaluation the spin polarization of a strong line ($^1D_2$, $^1G_4$ of the M_5 and M_4 components) dominates over the spin polarization of the less intense lines.

For comparison with theory, the measured spin polarization can be connected to the matrix elements of the decay processes via a parametrization which results from a purely kinematical consideration and is identical for photoelectrons and Auger electrons. For the transversal spin polarization component within the reaction plane we use [16]

$$P(\theta,\phi) = \frac{[2\xi P_{\mathrm{lin}} \sin 2\phi \mp (A + \alpha/2)\,|P_{\mathrm{circ}}|]\sin\theta}{1 - (\beta/4)[3\cos^2\theta - 1 - 3P_{\mathrm{lin}}\cos 2\phi \sin^2\theta]}\,. \quad (2)$$

The definition of the coordinate system can be seen from the inset to Fig. 1. The dynamical parameters β, ξ, and $A + \alpha/2$ denote the angular anisotropy, the dynamical spin polarization [17], and the transferred spin polarization, respectively, while $\mp$ corresponds to $\sigma^{\pm}$ light.

Since in our experiment $\phi = 45°$, the contribution of P_{lin} in the denominator vanishes. The P_{lin}-dependent term in the numerator vanishes, as we average over measurements taken with opposite helicities but constant linear component. P determined as such depends on P_{circ}, β, and $A + \alpha/2$ only. In the two-step model of Auger decay, i.e., the photoionization and Auger decay processes are assumed to proceed independently, the two latter quantities can be factorized into parameters describing the anisotropy of the primary hole state and into "intrinsic" parameters describing the Auger decay itself. The intrinsic parameters depend on the Auger matrix elements in a similar way as the photoionization dynamical parameters depend on the dipole matrix elements, hence giving detailed information about the electron-electron interaction which is governed by the Coulomb operator. Using the notation of [3] we get

$$(A + \alpha/2) = (\beta_1 - \gamma_1/2)A_{10} \quad \text{and} \quad \beta = -2\alpha_2 A_{20}\,. \quad (3)$$

A_{10} and A_{20} are the orientation and alignment parameters of the primary hole state and are proportional to its magnetic dipole moment and electric quadrupole moment, respectively [18]. β_1, γ_1, and α_2 are the intrinsic parameters. According to theory [3] A_{20} is small aside from the threshold region and any Cooper minimum. We therefore take the denominator in Eq. (2) as unity for the Auger lines. Using Eq. (3) and $\theta = 70°$ it follows

$$P = 0.94 P_{\mathrm{circ}}(\gamma_1/2 - \beta_1)A_{10}\,. \quad (4)$$

For transitions to a $^1S_0$ final ionic state the intrinsic parameters γ_1 and β_1 are fixed geometrical factors. Using $P/P_{\mathrm{circ}} = -0.39 \pm 0.06$ of the $M_4N_{4,5}N_{4,5}(^1S_0)$ line and the corresponding intrinsic parameters $\gamma_1 = 2/\sqrt{5}$ and $\beta_1 = -1/\sqrt{5}$ from [3] we determined the orientation of the $3d^{-1}\,{}^2D_{3/2}$ hole state to be $A_{10}^{\mathrm{Auger}} = -0.47 \pm 0.07$.

Additionally, the spin polarization $P/P_{\mathrm{circ}} = 0.67 \pm 0.09$ of the $3d_{3/2}$ photoline was used to determine the photoion orientation $A_{10}(3d_{3/2}^{-1})$ directly. Using the asymmetry parameter β from [19] and a nonrelativistic approximation [3,16] we obtain $A_{10}^{\mathrm{photo}} = -0.44 \pm 0.09$. The excellent agreement between A_{10}^{photo} and A_{10}^{Auger} is a strong evidence for the validity of the two-step model in this case. Table I presents the intrinsic parameters for all observed $M_{4,5}N_{4,5}N_{4,5}$ Auger lines extracted from the measured spin polarizations. While for the $3d_{3/2}^{-1}$ primary hole state A_{10}^{Auger} was used, for $3d_{5/2}^{-1}$ the nonrelativistic relation $A_{10}(3d_{5/2}^{-1}) = (28/27)^{1/2}A_{10}(3d_{3/2}^{-1})$ was applied [3].

So far no theoretical calculations of the intrinsic parameters for the Xe *MNN* Auger decay have been presented. However, we can compare qualitatively with published values for the Kr *MNN* Auger decay involving identical angular momentum states [3,20]. According to these calculations, Auger lines of the same final ionic state but emerging from primary hole states with opposite spin-orbit coupling, $d_{3/2}$ and $d_{5/2}$, have spin polarizations of

TABLE I. Intrinsic parameters $\gamma_1/2 - \beta_1$ for the Xe *MNN* Auger lines derived from the spin polarization data. For the $^1S_0$ line γ_1 and β_1 were taken from [3].

	$\gamma_1/2 - \beta_1$	
Final state	$M_4N_{4,5}N_{4,5}$	$M_5N_{4,5}N_{4,5}$
$^3F_4$	-0.18 ± 0.10	0.30 ± 0.06
$^3F_{2,3}$	-0.25 ± 0.05	-0.62 ± 0.08
$^3P_2$	-0.85 ± 0.19	0.30 ± 0.07
$^3P_{0,1}$	-0.23 ± 0.08	0.39 ± 0.12
$^1D_2$, $^1G_4$	0.69 ± 0.09	-0.71 ± 0.10
$^1S_0$	0.89	-0.88

opposite sign [with the exception of the Kr *MNN* ($^3P_2$) line]. A similar behavior can be observed in the Xe *MNN* case [Fig. 2(b)]: All the lines of the M_4 and M_5 groups exhibit opposite signs, with the exception of the $^3F_{2,3}$ double lines. This means that the positively spin polarized part of the $^3F_{2,3}$ double lines must dominate in both the M_4 and M_5 groups.

Besides the well known Auger lines additional intensity is obvious below 532 eV kinetic energy. Earlier investigations of the Xe *MNN* spectrum also recorded an enhanced, but unstructured intensity in this region [15,21,22]. This intensity may originate from a large number of $M_{4,5}O_i$-$N_{4,5}N_{4,5}O_i$ and $M_{4,5}N_i$-$N_{4,5}N_{4,5}N_i$ satellite Auger lines [22]. Since satellite processes are much weaker than the corresponding main processes, pronounced satellite effects should occur most clearly apart from main lines. Around 530 eV changes in the electron spin polarization can be seen [Fig. 2(b)]. The phenomenon certainly calls for a more detailed investigation.

In this Letter we presented spin dependent studies of the Xe *MNN* Auger group. We derived the orientation parameter A_{10} describing the polarization of the inner-shell hole independently from the photoelectron and Auger electron spin polarization data. The excellent agreement found between the two approaches confirms directly the two-step model of the Auger decay after inner-shell photoionization. The intrinsic Auger parameters describing the dynamics of the Auger process could be determined for the different *MNN* Auger lines within the two-step model. These results can be used to prove different angular momentum coupling models by comparison with theory.

Because of the low intensity of Auger lines and the resulting experimental difficulties of spin polarization analysis these measurements could succeed only by using a very effective spin-sensitive electron detector system and the high intensity, highly circularly polarized radiation of the ESRF helical undulator beam line. These new experimental tools certainly open up new perspectives for the spin-resolved Auger spectroscopy of atoms, molecules, solids, and surfaces.

We would like to thank the ERSF staff, especially J. Goedkoop and A. Rogalev, for the excellent working conditions. We are thankful to U. Kleineberg and H.-J. Stock for producing the multilayers and to R. David for testing the Mott polarimeter. This work was partly supported by the BMFT.

[1] U. Heinzmann and N. A. Cherepkov, in "VUV and Soft X-Ray Photoionization Studies," edited by U. Becker and D. A. Shirley (Plenum, New York, to be published).
[2] H. Klar, J. Phys. B **13**, 4741 (1980).
[3] N. M. Kabachnik and O. V. Lee, J. Phys. B **22**, 2705 (1989).
[4] U. Hahn, J. Semke, H. Merz, and J. Kessler, J. Phys. B **18**, L417 (1985).
[5] P. Stoppmanns, B. Schmiedeskamp, B. Vogt, N. Müller, and U. Heinzmann, Phys. Scr. **T41**, 190 (1992).
[6] R. Kuntze, M. Salzmann, N. Böwering, and U. Heinzmann, Phys. Rev. Lett. **70**, 3716 (1993).
[7] P. Elleaume, Nucl. Instrum. Methods Phys. Res., Sect. A **291**, 371 (1990); P. Elleaume, J. Synchrotron Radiat. **1**, 19 (1994).
[8] C. T. Chen, Nucl. Instrum. Methods Phys. Res., Sect. A **256**, 595 (1987); C. T. Chen and F. Sette, Rev. Sci. Instrum. **60**, 1616 (1989).
[9] L. G. Gray, M. W. Hart, F. B. Dunning, and G. K. Walters, Rev. Sci. Instrum. **55**, 88 (1984).
[10] S_{eff} was evaluated by comparing spin-resolved photoelectron spectra of Pt(111) obtained by a conventional Mott polarimeter [see A. Eyers *et al.*, Phys. Rev. Lett. **52**, 421 (1984)] and by the spherical Mott polarimeter used in this experiment.
[11] A. Kloidt, H.-J. Stock, U. Kleineberg, T. Döhring, M. Pröpper, K. Nolting, B. Heidemann, T. Tappe, B. Schmiedeskamp, U. Heinzmann, M. Krumrey, P. Müller, F. Scholze, S. Rahn, J. Hormes, and K. F. Heidemann, Proc. SPIE Int. Soc. Opt. Eng. **1742**, 593 (1992).
[12] R. Carr, J. B. Kortright, M. Rice, and S. Lidia, Rev. Sci. Instrum. **66**, 1862 (1995).
[13] We have shown at another undulator beam line for variable polarization that shifting the phase between two partial undulators for linear polarization does not change the total polarization [R. David, P. Stoppmanns, S.-W. Yu, R. Kuntze, N. Müller, and U. Heinzmann, Nucl. Instrum. Methods Phys. Res., Sect. A **343**, 650 (1994)]. Calculations of the light polarization of Helios I give a variation of P_{tot} of less than 1% if the phase is changed from $-\pi/2$ to $\pi/2$ (J. Chavanne and P. Elleaume, Internal Report No. ESRF-SR/ID-90-46; X. Marechal, Internal Report No. ESRF-SR/ID-91-50).
[14] M. Drescher, G. Snell, U. Kleineberg, H.-J. Stock, N. Müller, N. B. Brookes, and U. Heinzmann (to be published).
[15] L. O. Werme, T. Bergmark, and K. Siegbahn, Phys. Scr. **6**, 141 (1972).
[16] K.-N. Huang, Phys. Rev. A **22**, 223 (1980); **26**, 2274 (1982).
[17] Note that in [16] another quantity was termed ξ.
[18] K. Blum, *Density Matrix Theory and Applications* (Plenum Press, New York, 1981).
[19] U. Becker, H. G. Kerkhoff, M. Kupsch, B. Langer, D. Szostak, and R. Wehlitz, J. Phys. (Paris) Colloq. **48**, C9-497 (1987).
[20] B. Lohmann, U. Hergenhahn, and N. M. Kabachnik, J. Phys. B **26**, 3327 (1993); **27**, 1467 (1994).
[21] S. Aksela, H. Aksela, and T. D. Thomas, Phys. Rev. A **19**, 721 (1979).
[22] S. Hagmann, G. Hermann, and W. Mehlhorn, Z. Phys. **266**, 189 (1974).